Structure-properties relationship in ferromagnetic superconducting $RuSr_2GdCu_2O_8$

O. I. Lebedev* and G. Van Tendeloo
EMAT, University of Antwerp, Groenenborgerlaan 171, B-2020 Antwerpen, Belgium

G. Cristiani, H.-U. Habermeier, and A. T. Matveev
Max-Planck-Institut für Festkörperforschung, Heisenbergstrasse 1, D-70569 Stuttgart, Germany
(Received 23 November 2004; published 28 April 2005)

$RuSr_2GdCu_2O_8$ films with a different thickness are grown by pulsed laser deposition on a (100) STO substrate at 750 °C and an oxygen background pressure of 5×10^{-3} Pa. The film structure is characterized by x-ray diffraction, Raman spectroscopy and transmission electron microscopy (TEM), and correlated with the physical properties. All films exhibit ferromagnetic ordering at temperatures around 130 K, however not all films show superconductivity. TEM reveals that superconductivity in the films is related to the presence of an orthorhombic Ru-1212 phase with unit cell parameters $\sqrt{2}a_t\times\sqrt{2}a_t\times2c_t$. A model considering Cu substitution at Ru positions within the RuO_2 layer is proposed. The structure of the orthorhombic Ru-1212 with a doubled *c* axis can be described as a periodic alteration of superconducting $Ru_{1-x}Cu_xSr_2GdCu_2O_{8-\delta}$ layers and ferromagnetic $RuSr_2GdCu_2O_8$ layers. The structure in the thin film is strain induced, but there is a high probability that it will exist in bulk as well.

DOI: 10.1103/PhysRevB.71.134523 PACS number(s): 74.70.Pq, 68.60.Wm, 68.37.Lp

I. INTRODUCTION

After the discovery of high-T_C superconductivity in $YBa_2Cu_3O_{7-x}$ (Y-123),[1] the 123 family of superconducting cuprate compounds has been the subject of extensive research. Already early it was realized that their properties are closely correlated to the local structure and microstructure. This correlation of structural modifications with corresponding property changes served as a driving force in the search for new superconducting cuprates. Basically there are two major ways to induce structural modifications in the material. The first one is to alter the synthesis conditions by changing temperature and/or external pressure in order to stabilize a metastable structure or in the case of thin films to tailor the lattice mismatch or modify the substrate surface at a nanoscale[2] for controlled strain and/or defect generation. The second one is to apply (partial) chemical substitutions at cation and/or anion sites. Successive examples for Y-123 are as follows: replacing oxygen by fluorine;[3] replacing Y by other rare earth ions,[4] replacing Ba by Sr[5] or partially replacing Cu in the charge reservoir block by other small cations.[6] Bauernfeind *et al.*[7] reported a new class of compounds $RuSr_2LnCu_2O_8$ (Ln=Sm, Eu or Gd), noted as Ru-1212, where Cu-O chains are completely replaced by RuO_6 octahedra and Y is substituted by Sm, Eu or Gd. This structure was reported to be superconducting but not magnetic. Later, it was found that $RuSr_2GdCu_2O_8$ shows a remarkable coexistence of superconductivity (SC) ($T_C\approx48$ K) with ferromagnetic (FM) ordering of the Ru moments ($T_m\approx132$ K).[8] The SC has been attributed to the moment of the Cooper pairs in the CuO_2 planes, whereas the magnetic moments are located in the RuO_2 planes. The coexistence of superconductivity and magnetism, particularly ferromagnetism, has been a field of extensive theoretical and experimental investigations since decades initiated by the early paper of Ginzburg[9] showing an antagonistic nature of superconducting and ferromagnetic ordering. Later it was shown that SC can coexist with a FM phase[10] assuming an inhomogeneous structure (crystal, magnetic and electronic), a small magnetization in addition to disjoint FM and SC subsystems still allowing a coupling between them. This is realized in several *f*-electron compounds such as $R_xMo_6Se_8$ (R=Tb, Er, $x=1.0$ or 1.2),[11] $R_{1.2}Mo_6S_8$ (R=Tb, Dy, Er (Ref. 12)) and $ErRh_4B_4$.[13] In non-BCS triplet superconductors where electron pairing is magnetically mediated, superconducting ordering in the ferromagnetic phase is less unlikely than in the single superconductor. It is thought that this situation is realized in UGe_2[14] and $ZrZn_2$,[15] though there is still some controversy.[16] As far as the cup rate superconductors are concerned, no mixing of superconductivity and antiferromagnetism was concluded based on recent experiments on SC/AFM/SC trilayer junctions.[17]

Recently several reports claim the coexistence of SC and FM in the ruthenocuprates[18,19] and a tuning of their properties by doping.[20–22] Reports of both superconducting and nonsuperconducting Ru-1212 have triggered experimental studies to investigate the structural origin of superconductivity (or nonsuperconductivity) in this material. Structure determination is mainly based on (synchrotron) x-ray powder diffraction[23] and neutron diffraction.[24,25] However, some of the data are contradictory and a matter of discussion. We therefore decided to carefully investigate the structure of Ru-1212 on a local scale and compare the microstructure of superconducting and nonsuperconducting Ru-1212. A combination of transmission electron microscopy (TEM) with Raman spectroscopy and (conventional) XRD is very powerful and will allow us not only to focus on the average changes observed by Raman and XRD, but also on the local changes in structure and microstructure. Indeed, some microstructure changes are too small to lead to observable effects in XRD and Raman. Up to now only a few TEM based studies of the microstructure properties of Ru-1212 have been reported[26,27] and none of them correlates the micro-

structure with transport and/or magnetic properties.

In the present contribution we have studied $RuSr_2GdCu_2O_8$ thin films and we focus on the structural differences between superconducting and nonsuperconducting Ru-1212 films prepared under comparable growth conditions.

II. EXPERIMENT

$RuSr_2GdCu_2O_8$ films with different thicknesses were synthesized in a two step process on single crystal (100)-oriented $SrTiO_3$ substrates (100-STO) by pulsed laser deposition (PLD) using a ceramic disk-shaped stoichiometric $RuSr_2GdCu_2O_8$ target. The beam of a KrF excimer laser ($\lambda = 248$ nm) was focused on the target to yield a fluency of ~ 2 J/cm^2. For the deposition of the precursor films a substrate temperature of 750 °C and an oxygen background pressure of 5×10^{-3} Pa were used. Subsequently, the films were annealed at 1000 °C in flowing Ar for 1 h and then in oxygen at 1040 °C $< T_{an} <$ 1060 °C. To improve purity and crystallinity one film (RG84) was prepared via successive deposition and the crystallization of two layers 200 nm thick. Details on the synthesis procedure as well as on the film characterization are published elsewhere.[28] In the present study we investigated samples denoted in Ref. 28 as series "*h*." All films exhibit ferromagnetic ordering at temperatures around T_m (see Table I), however not all films show superconductivity.

The x-ray diffractometry was done on Cu K_α radiation by a Philips PW 3710 diffractometer equipped with a curved C monochromator on a diffracted beam. Raman spectroscopy was performed at room temperature with unpolarized light of 514.5 nm using a Dilor triple-grating spectrometer equipped with a liquid nitrogen cooled CCD detector. Resistance measurements were carried out at 10 μA of AC with four thermally evaporated Au/Cr stripe electrodes. Cross-section and plan-view specimens for TEM were prepared by mechanically grinding to a thickness of about 10 micron, followed by final ion-beam milling in a Balzers REP 010 machine. TEM investigations were carried out with a JEOL 4000EX microscope. The Mac Tempas/CrystalKit software is used for computer simulating the experimental HREM images.

The phase composition of the domains, and, in particular, the Ru:Sr:Gd:Cu ratio, was determined by energy dispersive x-ray analysis (EDX) in a Philips CM20 microscope with a LINK-2000 attachment. The electron probe size is in the nanometer range and is much smaller than the crystal size. It therefore provides reliable chemical information on a single crystal domain. The experimental cation ratio, as determined by EDX taken from 10 domains (Ru:Sr:Gd:Cu $= 0.152:0.32:0.165:0.363$), is very close to the expected composition for $Ru_1Sr_2GdCu_{2+x}O_{8-\delta}$ with some excess of Cu ($x \approx 0.33$) and a slight Ru deficiency. ICP-AES data from as deposited precursor films gave similar results.

III. STRUCTURAL DATA

The crystal structure of the $SrTiO_3$ substrate is cubic perovskite ($Pm3m$) with lattice parameter $a = 0.39050$ nm.

$RuSr_2GdCu_2O_8$ (Ru-1212) is structurally related to $YBa_2Cu_3O_{7-x}$ with Y, Ba, and Cu(1) being replaced by Gd, Sr and Ru, respectively. However, it contains corner-sharing RuO_6 octahedra substituting for the Cu-O chains. The structure is tetragonal with space group $P4/mmm$ (*123*) and lattice parameters $a = 0.383\,84$ nm, $c = 1.1573$ nm.[23] The Ru atoms occupy octahedral sites and are surrounded by six oxygen atoms: four equatorial atoms *(O1)* and two apical ones (*O4*). Chimaissem *et al.*[24] however reported neutron powder diffraction data for $RuSr_2GdCu_2O_8$ where weak superlattice lines indicated a $\sqrt{2}a_p \times \sqrt{2}a_p \times c$ cell as a result of the RuO_6 octahedra tilting. Their model is described by a tetragonal space group $P4/mbm$ *(127)* with unit cell parameters $a = 0.542\,49$ nm, $c = 1.156\,28$ nm.

IV. RESULTS

A. X-ray diffraction

X-ray diffraction analysis[28] has shown that samples RG52, RG53, RG54 contain (001) oriented Ru-1212 grains with a lattice parameter $c = 11.51(8)$ Å, but also ($hh0$) oriented Sr_2GdRuO_6 (2116) grains, and Gd_2CuO_4 (214) with a preferential grain orientation of ($h00$). The overall amount of impurities, roughly estimated from x-ray peak intensities, is about 35% and is minimal in the sample RG52. The RG84 sample is nearly single phase (001) oriented Ru-1212 with a c parameter of 11.57(9) Å; only a small amount of impurities is seen in the XRD pattern.

B. Electrical transport measurements

The temperature dependence of the resistance of the films is shown in Fig. 1(a). The resistance of the RG52, RG53, and RG54 samples has a metallic behavior in a range of 130–300 K and a semiconducting behavior between 30 and 130 K; this is typical for underdoped high-T_c superconductors. At $\sim$30 K the resistance of the RG52 sample strongly drops, suggesting the onset of a superconducting transition, though it does not reach zero down to 5 K. The onset temperature of RG53 is $\sim$25 K and the transition is broadened. RG54 film only shows a weak indication for the transition. RG84 has a semiconducting temperature dependence of the resistance.

C. Raman spectroscopy

The Raman spectra of the samples with a subtracted substrate signal are shown in Fig. 1(b). The spectra of the samples coincide with that of the Ru-1212 phase with an additional band observed around 529 cm^{-1} (between 460–600 cm^{-1}) and a peak at 761 cm^{-1}. The band apparently originates from the film-substrate interface. The peak at 761 cm^{-1} is associated with the Sr_2GdRuO_6 compound because this peak is observed only in the samples (RG52, RG53, RG54) containing the (2116) phase and it is not seen in the spectra of RG84. However, we cannot explain the strong hardening of this phonon mode in our samples in comparison with the reported line position of $\sim$720 cm^{-1} for the Sr_2GdRuO_6 phase.[29] We observed no difference in Raman spectra (such as peak positions, peak broadness or rela-

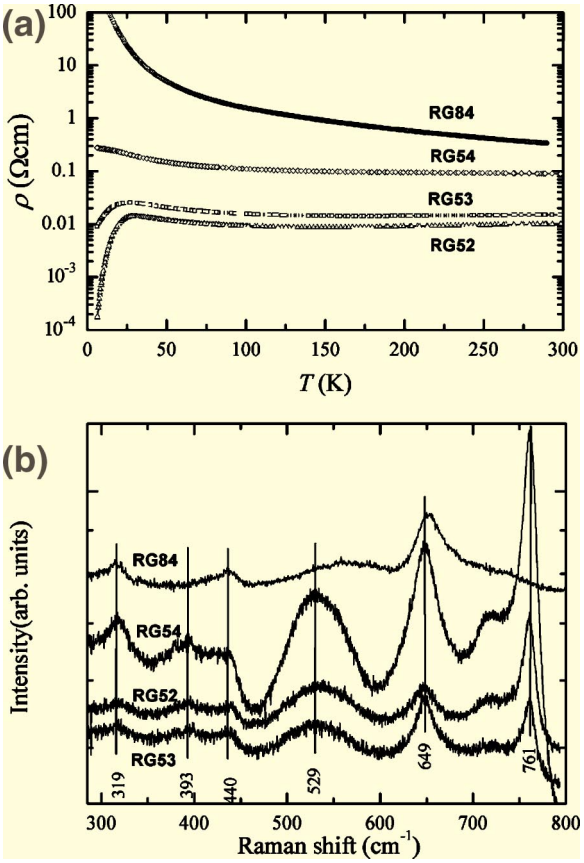

FIG. 1. (a) Temperature dependence of the resistance of RG52, RG53, RG54, RG84 films. (b) Raman spectra of the films with a subtracted substrate signal.

tive intensities) between the superconducting samples (RG52, RG53) and the nonsuperconducting ones (RG54, RG84).

D. Electron microscopy

The exact structure as well as the microstructure of the different Ru-1212 films is a crucial point. Electron diffraction (ED) together with HREM from two orthogonal directions (plan view and cross section) provides essential information for the structural analysis. Moreover, EDX data allow a chemical identification, particularly on the cation ratio.

Cross-section images of the most representative films (RG84 and RG52) with different thicknesses (400 nm and 1500 nm) are shown in Fig. 2. The thinnest film (Fig. 2(a)) exhibits an island structure; the coverage of the substrate is partial and all islands grow epitaxially with a fixed orientation to the substrate surface. HREM images (Fig. 3) clearly show that the Ru-1212 islands are perfectly coherent across the interface with the *c* axis parallel to the interface normal. The microstructure of the films changes with thickness and the films adopt a granular structure at a thickness >1000 nm (Fig. 2(b)). Occasionally impurity phases, identified as $SrCuO_3$ and Sr_2RuO_4,[30] were detected by a combination of TEM and EDX. $SrCuO_3$ is not superconducting and therefore does not influence the superconducting properties

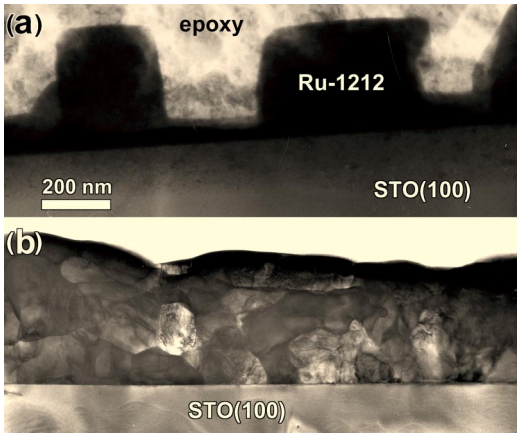

FIG. 2. Cross-section bright field images of Ru-1212 films with a thickness of 400 nm (a) and 1.5 μm (b) on a STO(100) substrate.

of the film. Sr_2RuO_4 is believed to be a spin triplet superconductor, however, with a T_c as low as 1.5 K, anyway, much lower than that of the investigated film and therefore it cannot be responsible for the superconducting properties of the film. The size of the Ru-1212 domains is varying from 50 nm to 500 nm and increases with film thickness.

The [100] selected area ED pattern in Fig. 4(b) shows the presence of 90 deg twins or mirror twins. Because of the pseudocubic structure of the tetragonal Ru-1212, twinning is to be expected; such twins have previously been observed in bulk material.[31] All ED patterns of RG 54 or RG 84 (Figs. 4(a) and 4(b)) can be indexed with reference to the tetragonal $P4/mmm$ space group. The weak reflections in the center of the square mesh of the ED pattern in Fig. 4(b) are the result of double diffraction related to the presence of twin interfaces.

In the ED patterns of the superconducting RG 52 and RG 53 films, additional weak reflections are observed in the

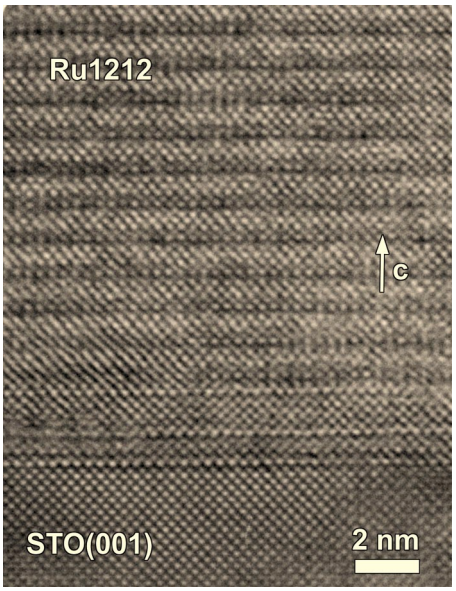

FIG. 3. Cross-section HREM image of a Ru-1212 island (Fig. 2(a). The film is *c* oriented.

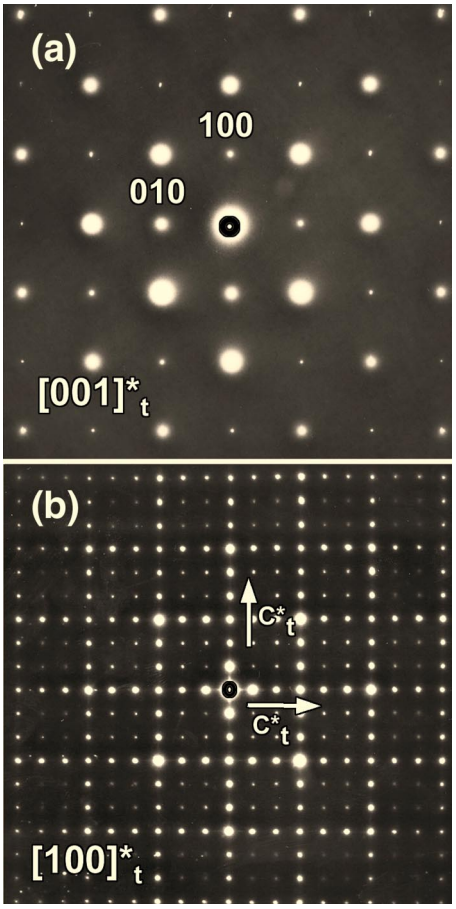

FIG. 4. Diffraction patterns of the Ru-1212 structure along two relevant zones: (a) $[001]_t$ and (b) $[100]_t$ indexed with respect to the $P4/mmm$ space group. The [100] pattern is due to the presence of two orientation variants with mutually perpendicular c axis.

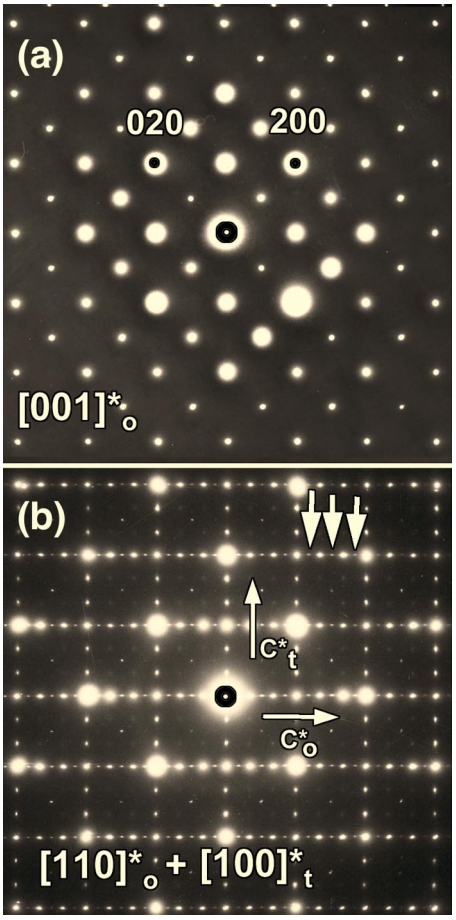

FIG. 5. Diffraction patterns of a Ru-1212 structure along two relevant zones: (a) $[001]_O$ and (b) $[110]_O$ indexed with respect to the *Pbam* space group. Note the weak superstructure spots marked by arrowheads.

$[001]^*$ pattern; they correspond to the $\sqrt{2}a_t \times \sqrt{2}a_t$ superstructure.[23,24] In the $[100]_t$ cross section pattern (Fig. 5), a twinned structure is also present, but the set of reflections along two mutually perpendicular directions (indicated c^*_o and c^*_t) is different. Grains with their c axis parallel to the interface exhibit extra superstructure spots while grains with their c axis perpendicular to the interface show the "regular" reflections. The superstructure spots, indicated by arrows in Fig. 5(b), are positioned at $(0, 0, l/2)$ and suggest a doubling of the c parameter. Together with the diffraction conditions of $P4/mbm$ *(127)* this leads to a new unit cell with parameters $\sqrt{2}a_t \times \sqrt{2}a_t \times 2c_t$. The other 90 deg rotated ED pattern (along c^*_t in Fig. 5) either belongs to the tetragonal $P4/mmm$ space group with an $a_t \times a_t \times c_t$ cell or to the tetragonal $P4/mbm$ with $\sqrt{2}a_t \times \sqrt{2}a_t \times c_t$.[23,24] Careful analysis of the [001] ED pattern in Fig. 5(a) shows that the pattern is not square but has a very small orthorhombic distortion ($a/b \approx 1.01$). The splitting of high order reflections in Fig. 5(b) also suggests that the difference between the twin domains is not only in the doubling of the c axis, but that also slight lattice parameter changes are involved. All these data strongly suggest that the diffraction pattern is a superposition of two 90 deg rotated patterns produced by a tetragonal structure and an orthorhombic structure. The actual orthorhombic space group is most probably a maximal subgroup of $P4/mbm$, which has to satisfy the following diffraction conditions: $0kl$, $k=2n$; $h0l$, $h=2n$; $h00$, $h=2n$; $0k0$, $k=2n$. This points towards an orthorhombic *Pbam (55)* space group with unit cell $a_o \approx \sqrt{2}a_t$; $b_o \approx \sqrt{2}a_t$; $c_o \approx 2c_t$.

An HREM image of the orthorhombic Ru-1212 domain along $[001]_O$ is shown in Fig. 6. The image simulation, based on the orthorhombic *Pbam (55)* space group, is given as an inset in Fig. 6 and shows a good agreement between the experimental and the calculated image. It should be mentioned that this orthorhombic structure is only present in the superconducting RG 52 and RG53 films; not in the RG84 and RG54 films.

$[110]_O$ HREM observations confirm the doubling of the c axis (Fig. 7). As mentioned before, this period doubling only appears in domains with the c axis parallel to the substrate (Fig. 7). The period doubling along the c axis is apparently related to the fact that successive RuO_2 layers are no longer equivalent, and they are imaged with a different contrast. Simulated images (using a model based on the $P4/mbm$ structure) indeed show that the brighter rows correspond to the RuO_2 layers.

At the interface between substrate and domains with the c axis parallel to the interface (white arrows in Fig. 7), an

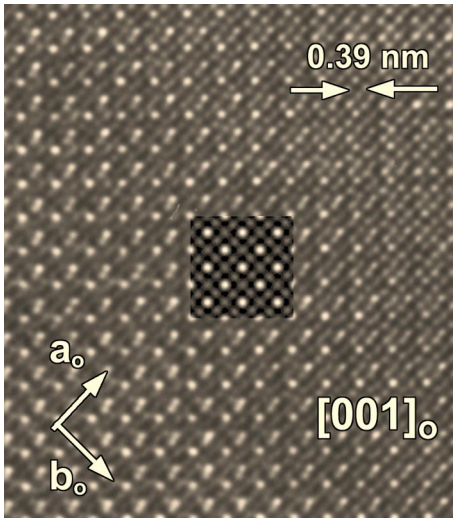

FIG. 6. HREM image of a Ru-1212 domain along $[001]_O$. The inset shows a simulated image based on the orthorhombic *Pbam* space group.

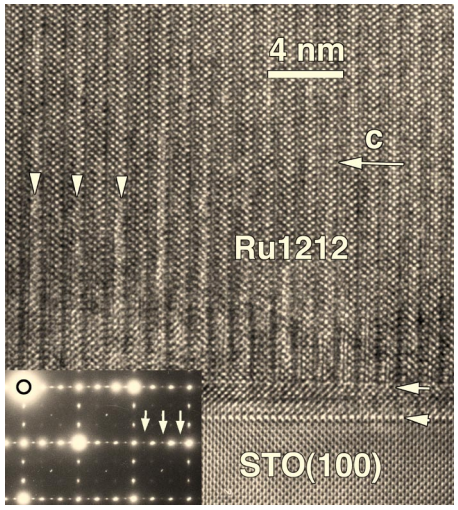

FIG. 7. Cross-section HREM image along $[110]_O$ of a domain with the *c* axis parallel to the interface. The corresponding ED pattern is also shown. Note the weak double periodicity contrast marked by vertical white arrows.

intermediate layer, several unit cells thick, is observed. The layer is about 2 nm wide and seems to have a cubic structure along the viewing direction. No further analysis of this layer was performed.

When domains are oriented with their *c* axis normal of substrate, no superstructure is observed and the contrast is typical for the regular tetragonal Ru-1212 phase (cf. Fig. 3). For both domain orientations, film and substrate are perfectly coherent, no misfit dislocations being formed, and the interfaces are sharp and well defined.

V. DISCUSSION

Our experiments provide us with the following information:

(a) Superconducting as well as nonsuperconducting ferromagnetic Ru-1212 films can be grown on a STO substrate; all superconducting films contain the new orthorhombic Ru-1212 phase ($a_o = \sqrt{2}a_t$; $b_o = \sqrt{2}a_t$; $c_o = 2c_t$); the nonsuperconducting do not.

(b) Image simulations of the Ru-1212 structure, based on the tetragonal $P4/mbm$ model, reveal that the distortions related to the formation of the new superstructure are primarily located in the RuO_2 layers.

(c) The appearance of the $1/2[001]$ superstructure depends on the orientation of the domains with respect to the substrate surface. Only domains oriented with the *c* axis parallel to the substrate exhibit a doubling along the *c* axis.

(d) The composition of orthorhombic phase with the $1/2[001]$ superstructure corresponds to the Ru-1212 phase with some excess of Cu.

These experimental facts strongly suggest that superconductivity in the ferromagnetic Ru-1212 films is directly related to the structure of the film. All films are ferromagnetically ordered and contain the tetragonal Ru-1212 phase. Therefore, ferromagnetism can be unambiguously attributed to the tetragonal Ru-1212 phase. The only difference between superconducting and nonsuperconducting films is the presence of the orthorhombic Ru-1212 structure in the superconducting films. Therefore it seems reasonable to attribute superconductivity to the orthorhombic Ru-1212 phase with a doubled *c* axis and with a slight Cu excess.

Superlattice lines, defining a $\sqrt{2}a_t \times \sqrt{2}a_t \times c_t$ unit cell, have been observed by neutron powder diffraction[24] and they have been explained by a rotation in the opposite sense of the RuO_6 octahedra, leading to an ordered arrangement of the distortions. McLaughlin *et al.*[23] reported HREM evidence of this superstructure in bulk Ru-1212 material. However none of these research groups reported a doubling along the *c* axis. The reason why they missed this doubling probably has to do with the high density of twins and the limitations of the powder technique for x rays as well as for neutrons. Another reason could be that in bulk material, these structural features are less pronounced. In a thin film, the substrate structure and the surface orientation impose a specific epitaxial relation that can induce a different type of deformation in the film structure.[31,32] In the present case a doubling of the *c* parameter is only found when the *c* axis is oriented parallel to the substrate surface. Since STO has a cubic structure, it is logical that a tetragonal structure is favored with the *c* axis oriented normal to the substrate and with $(001)_t$ as the contact plane. In this case the misfit strain is minimal. However, as soon as the structure exhibits an orthorhombic distortion in the *ab* plane ($a \neq b$), there is no longer a symmetry similarity between STO and the $(001)_O$ contact plane, but the $(110)_O$ plane still maintains a pseudocubic symmetry ($a \approx c/3$). This favors the growth of the orthorhombic structure with the *c* axis parallel to the substrate.

Obviously, the difference between the tetragonal and the orthorhombic Ru-1212 structure is a different rotation scheme of the RuO_6 octahedra.[23,24] To explain the double period two models can be proposed.

First, an orthorhombic structure can be simply obtained by a shear displacement of the apical O4 oxygen atoms to-

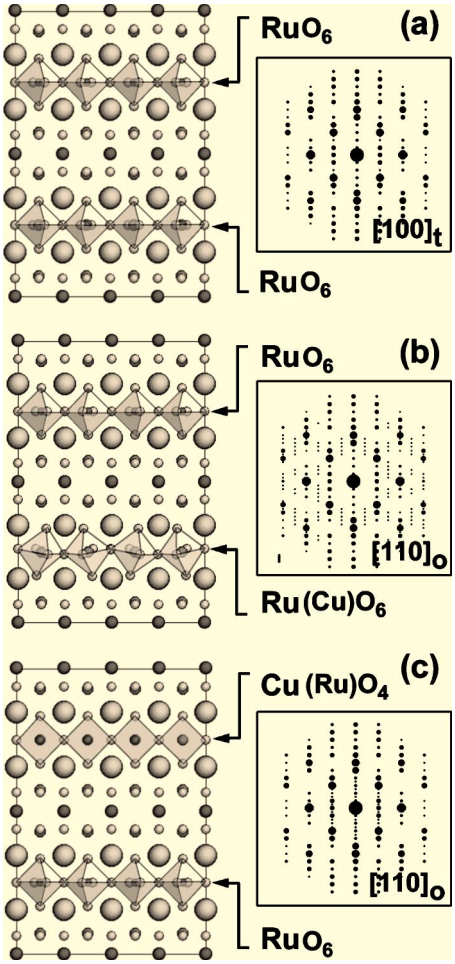

FIG. 8. A comparison of possible structure and the corresponding calculated ED patterns of Ru-1212 structures based on a different RuO_2 layer arrangement: (a) $[100]_t$ zone view of the tetragonal $RuSr_2GdCu_2O_8$ structure; (b) $[110]_O$ view of an orthorhombic distorted $Ru(Cu)Sr_2GdCu_2O_8$ structure induced by a different tilting of the RuO_6 octahedra in alternating layers; (c) $[110]_O$ view of an orthorhombic distorted $Ru_{1-x}Cu_xSr_2GdCu_2O_8$ structure induced by substitution of a RuO_2 plane by a CuO chain in alternating layers.

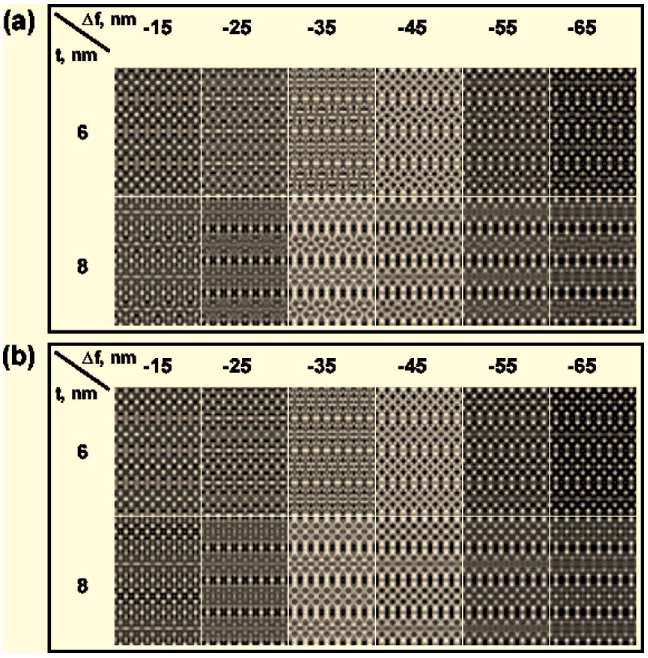

FIG. 9. Matrix of simulated images of the Ru-1212 structure based on the models proposed in Figs. 8(b) and 8(c), respectively.

gether with a displacement of the O1 oxygen atoms out of the plain. A difference in the sense of the rotation of the RuO_6 octahedra along the *c* direction then leads to a doubling of the *c* parameter. The question however remains why successive RuO_2 layers would have a different geometric configuration. Our experimental data do not give a unique answer, but some data allow us to exclude certain models. Taking into account that Ru has the ability to adopt two different ionization states:[33] Ru^{5+} and Ru^{4+}, one might assume that the oxygen coordination octahedral, associated with these differently charged ions, have a different shape. The strain induced by the substrate could influence the elastic interaction between deformed octahedra and an ordering of the rotation of the RuO_6 octahedra along the *c* axis could be favored (Fig. 8(b)). This ordering could be considered as a charge ordering of Ru^{5+} and Ru^{4+}. HREM image simulations based on this model are presented in Fig. 9(a) and exhibit the main features of the experimental images. However, an ordering of the rotation of the RuO_6 octahedra not only leads to a doubling of the *c* parameter but also to the appearance of superstructure spots along other crystallographic directions, e.g., in the $[110]_O$ zone (see the simulated ED pattern of Fig. 8(b)). Definitely, this superstructure was never observed experimentally. Moreover, this model does not take into account the small excess of Cu (according to EDX $\delta \approx 0.33$) in the orthorhombic ordered phase. The absence of any visible difference in Raman spectra, which should be sensitive to RuO_6 octahedra displacements, also argues against this model.

A second model is suggested by the ability of Cu to occupy the Ru site positions[21,22,26] and the fact that the physical properties strongly depend on the sample preparation. It is well known that the synthesis of single phase Ru-1212 is far from easy. One of the main reasons is that Ru-1212 undergoes a solid phase decomposition at a relatively low temperature ($\sim$1060 °C in oxygen and $\sim$1040 °C in air[34–36]). This and the necessity of a high temperature treatment to achieve the structural ordering required for superconductivity[23,24] can lead to domain formation and the formation of secondary phases. Diffusion along the domain boundaries is much easier and can challenge the growth of a secondary phase at the grain boundaries.[16] For thin films, the epitaxial stress and the imposed substrate orientation are extra parameters. It is therefore difficult to exclude that in Ru-1212 samples substitution of Ru by Cu would take place. Ru substitution by Cu can lead to an oxygen rearrangement around the Ru(Cu) site and create Cu chains instead of RuO_2 planes (Fig. 8(c)). The replacement of a RuO_2 square planar layer (not considering the apical oxygen!) by CuO chains will induce an orthorhombic distortion in the Ru-1212 structure similar to the one in $YBa_2Cu_3O_{7-x}$. Moreover, recently superconductivity has been reported in $Ru_{1-x}Cu_xSr_2GdCu_2O_{8-\delta}$ at a T_c as high as 74 K.[21,22] A real-

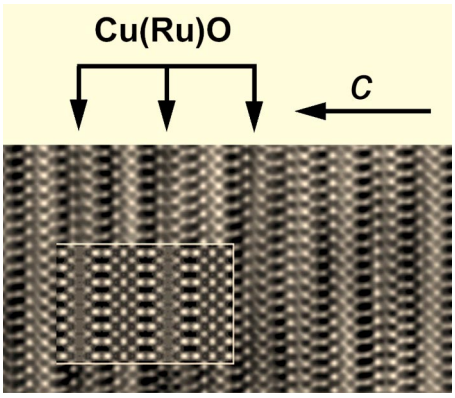

FIG. 10. Filtered $[110]_O$ experimental HREM image. The inset shows the simulated image based on the model of Fig. 8(c) (defocus—55 nm and thickness 8 nm).

istic model for the superstructure will assume a partial substitution of Ru by Cu and a random distribution of the Cu along the layer. The model proposed in Fig. 8(c) and image simulations based on this model (Fig. 9(b)) were made for a 50% Cu–50% Ru distribution within the layer. The total Cu stoichiometry would then be 2.25, close to the experimental EDX data (2.33). The image simulation based on the proposed model for $Ru_{1-x}Cu_xSr_2GdCu_2O_{8-\delta}$, $x=0.25$ (Fig. 9(b)) superimposed on the HREM image of Fig. 10 shows a good agreement between calculation and experiment.

Ru-1212 with the doubled *c* axis can now be interpreted as a sandwich of two slabs: superconducting/nonsuperconducting and can be described as a succession of layers $Ru_{1-x}Cu_xSr_2GdCu_2O_{8-\delta}-RuSr_2GdCu_2O_{8-\delta}-\cdots$. In other words, the Ru-1212 structure contains, alternating along the *c* direction, RuO_6 (FM) and $Cu_{1-x}Ru_xO_{6-\delta}$ (SC) layers (Fig. 8(c)).

A model considering Cu substitution at the Ru positions along the *b* direction, leading to formation of superconducting-normal-superconducting (SNS) junctions has been previously proposed.[26] However, no evidence for Cu ordering within the RuO_2 layer was found. Our model may also explain the broadening of the resistivity transition for Ru-1212 (Fig. 1).

VI. CONCLUSIONS

The transport and magnetic properties and their correlation with the microstructure have been investigated for $RuSr_2GdCu_2O_8$ films grown on a (100) $SrTiO_3$ single crystal substrate. It has been shown that for the Ru-1212 films superconductivity is related to the presence of an orthorhombic $Ru_{1-x}Cu_xSr_2GdCu_2O_{8-\delta}$ phase with unit cell parameters $\sqrt{2}a_t\times\sqrt{2}a_t\times 2c_t$. The doubling of the *c* parameter is the result of a different structure in alternating RuO_2 planes. Several models based on different tilting schemes of the RuO_6 octahedra and possible substitutions of Ru by Cu have been considered and a model satisfying all experimental data has been proposed. For the present Ru-1212 thin films, superconductivity is related to a sandwich type structure containing two subunit phases: superconducting $Ru_{1-x}Cu_xSr_2GdCu_2O_{8-\delta}$ and ferromagnetic $RuSr_2GdCu_2O_8$ layers.

ACKNOWLEDGMENTS

This work has been performed within the framework of the IAP V-I project of the Belgian government.

*Author to whom correspondence should be addressed.

[1] M. K. Wu, J. R. Ashburn, C. J. Torng, P. H. Hor, R. L. Meng, L. Gao, Z. J. Huang, Y. Q. Wang, and C. W. Chu, Phys. Rev. Lett. **58**, 908 (1987).
[2] J.-P. Locquet, J. Perret, J. Fompeyrine, E. Machler, J. W. Seo, and G. VanTendeloo, Nature (London) **394**, 453 (1998)
[3] R. V. Spanchenko, M. G. Rozova, A. M. Abakumov, E. I. Ardashnikova, M. L. Kovba, S. N. Putilin, E. V. Antipov, O. I. Lebedev, and G. Van Tendeloo, Physica C **280**, 272 (1997).
[4] A. del Moral, M. R. Ibarra, P. A. Algarabel, and J. I. Arnaudas, Physica C **161**, 48 (1989).
[5] O. I. Lebedev, G. Van Tendeloo, F. Licci, E. Gilioli, A. Gauzzi, A. Prodi, and M. Marezio, Phys. Rev. B **66**, 132510 (2002).
[6] A. T. Matveev, Y. Matsui, S. Yamaoka, and E. Takayama-Muromachi, Physica C **288**, 185 (1997).
[7] L. Bauernfeind, W. Widder, and H. F. Braun, Physica C **254**, 151 (1995).
[8] J. L. Tallon, C. Bernhard, M. E. Bowden, P. M. Gilberd, T. M. Stoto, and D. J. Pringle, IEEE Trans. Appl. Supercond. **9**, 1696 (1999).
[9] V. L. Ginzburg, Sov. Phys. JETP **4**, 153 (1957).
[10] P. W. Anderson, H. Suhl, Phys. Rev. **116**, 898 (1959).
[11] R. W. McCallum, D. C. Johnston, R. N. Shelton, W. A. Fertig, and M. B. Maple, Solid State Commun. **24**, 501 (1977).
[12] M. Ishikawa and Ø. Fisher, Solid State Commun. **24**, 747 (1977).
[13] W. A. Fertig, D. C. Johnston, L. E. DeLong, R. W. McCallum, M. B. Maple, and B. T. Matthias, Phys. Rev. Lett. **38**, 987 (1977).
[14] S. S. Saxena, P. Agarwal, K. Ahilan *et al.*, Nature (London) **406**, 587 (2000).
[15] C. Pfleiderer, M. Uhlarz, S. M. Hayden *et al.*, Nature (London) **412**, 58 (2001).
[16] Y. Zhou, J. Li, and Cg-De Gong, Solid State Commun. **132**, 507 (2004).
[17] I. Bozovic, G. Logvenov, M. A. Verhoeven, P. Caputo, E. Goldobin, and T. H. Geballe, Nature (London) **422**, 873 (2003).
[18] C. Bernhard, J. L. Tallon, C. Niedermayer, T. Blasius, A. Golnik, E. Brücher, R. K. Kremer, D. R. Noakes, C. E. Stronach, and E. J. Ansaldo, Phys. Rev. B **59**, 14 099 (1999).
[19] W. E. Pickett, R. Weht, and A. B. Shick, Phys. Rev. Lett. **83**, 3713 (1999).
[20] A. C. McLaughlin and J. P. Attfield, Phys. Rev. B **60**, 14 605 (1999).
[21] P. W. Klamut, B. Dabrowski, S. Kolesnik, M. Maxwell, and J. Mais, Phys. Rev. B **63**, 224512 (2001).

[22] P. W. Klamut, B. Dabrowski, S. M. Mini, M. Maxwell, J. Mais, I. Felner, U. Asaf, F. Ritter, A. Shengelaya, R. Khasanov, I. M. Savic, H. Keller, A. Wisniewski, R. Puzniak, I. M. Fita, C. Sulkowski, and M. Matusiak, Physica C **387**, 33 (2003).
[23] A. C. McLaughlin, W. Zhou, J. P. Attfield, A. N. Fitch, and J. L. Tallon, Phys. Rev. B **60**, 7512 (1999).
[24] O. Chmaissem, J. D. Jorgensen, H. Shaked, P. Dollar, and J. L. Tallon, Phys. Rev. B **61**, 6401 (2000).
[25] J. D. Jorgensen, O. Chmaissem, H. Shaked, S. Short, P. W. Klamut, B. Dabrowski, and J. L. Tallon, Phys. Rev. B **63**, 054440 (2001).
[26] V. P. S. Awana, S. Ichihara, J. Nakamura, M. Karppinen, H. Yamauchi, J. Yang, W. B. Yelon, W. J. James, and S. K. Malik, J. Appl. Phys. **91**, 8501 (2002).
[27] T. Yokosawa *et al.*, Ultramicroscopy **98**, 283 (2004).
[28] A. T. Matveev, G. Cristiani, E. Sader, V. Damljanoviç, and H.-U. Habermeier, Physica C (to be published).
[29] A. Fainstein, A. E. Pantoja, H. J. Trodahl, J. E. McCrone, J. R. Cooper, G. Gibson, Z. Barber, and J. L. Tallon, Phys. Rev. B **63**, 144505 (2001).
[30] Q. Huang, J. L. Soubeyroux, O. Chimaissen, I. Natali Sora, A. Santoro, R. S. Cava, J. J. Krajewski, and W. F. Peck, J. Solid State Chem. **112**, 355 (1994).
[31] O. I. Lebedev, G. Van Tendeloo, S. Amelinckx, B. Leibold, and H.-U. Habermeier, Phys. Rev. B **58**, 8065 (1998).
[32] M. D. Rossel, A. M. Abakumov, G. Van Tendeloo, J. A. Pardo, and J. Santiso, Chem. Mater. **16**, 2578 (2004).
[33] R. S. Liu, L.-Y. Jang, H.-H. Hung, and J. L. Tallon, Phys. Rev. B **63**, 212507 (2001).
[34] A. T. Matveev, A. Kulakov, A. Maljuk, C. T. Lin, and H.-U. Habermeier, Physica C **400**, 53 (2003).
[35] A. T. Matveev, E. Sader, V. Duppel, A. Kulakov, A. Maljuk, C. T. Lin, and H.-U. Habermeier, Physica C **403**, 231 (2004).
[36] A. T. Matveev, A. N. Maljuk, A. Kulakov, C. T. Lin, and H.-U. Habermeier, Physica C **407**, 139 (2004).